Electronic Supplementary Material (ESI) for Journal of Materials Chemistry A.

Supporting Information

Defect-typed AlO_x nanointerface boosting layered Mn-based oxide cathode for wide-temperature sodium-ion battery

Zelin Ma [a], *Hanxue Xu* [a], *Yunxuan Liu* [a], *Qian Zhang* [a], *Mengtong Wang* [a], *Yuchen Lin* [a], *Zhuo Li* [a], *Xuexia He* [a], *Jie Sun* [a], *Ruibin Jiang* [a], *Zhibin Lei* [a], *Qi Li* [a,]*, *Longhai Yang* [b,]* *and Zong-huai Liu* [a]

a. Key Laboratory of Applied Surface and Colloid Chemistry, Shaanxi Normal University, Ministry of Education, Xi'an, 710062, P. R. China; School of Materials Science and Engineering, Shaanxi Normal University, Xi'an, 710119, P. R. China.

b. School of Electrical and Control Engineering, Xi'an University of Science and Technology, Xi'an 710054, Shaanxi, P.R. China.

* Corresponding author.

E-mail: clliqi@snnu.edu.cn and ylonghai@hotmail.com.

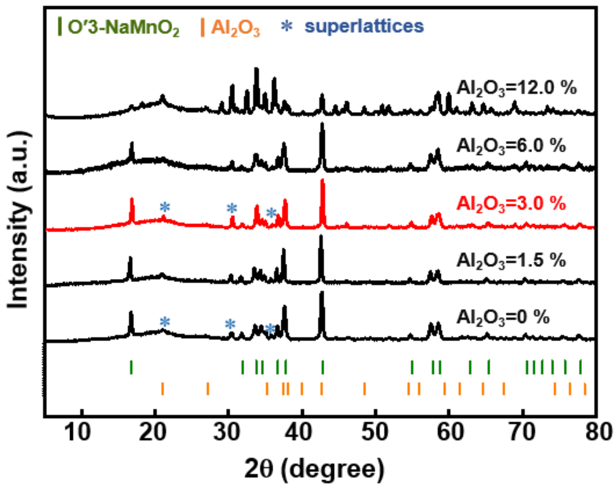

Figure S1. XRD patterns of NMA@AlO$_x$ samples prepared on basis of the different additional Al_2O_3 contents.

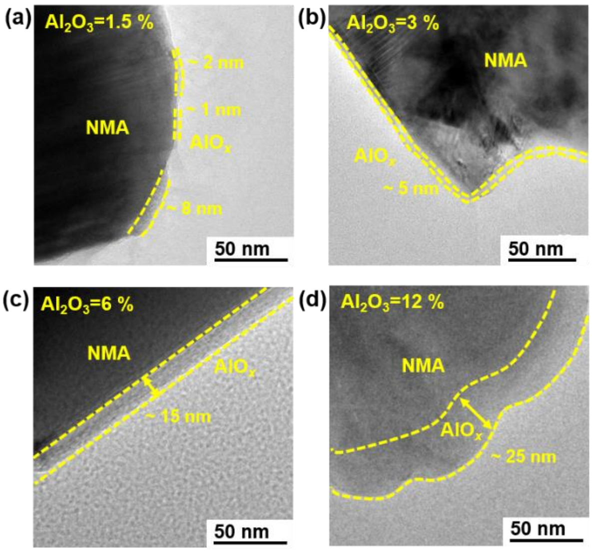

Figure S2. TEM images of NMA@AlO_x samples prepared on basis of the different additional Al_2O_3 contents.

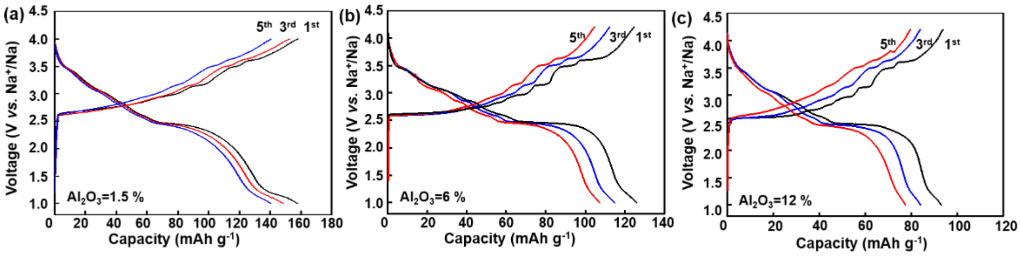

Figure S3. Charge and discharge curves of Na/NMA@AlO$_x$ cells based on the utilization of the different additional Al_2O_3 contents.

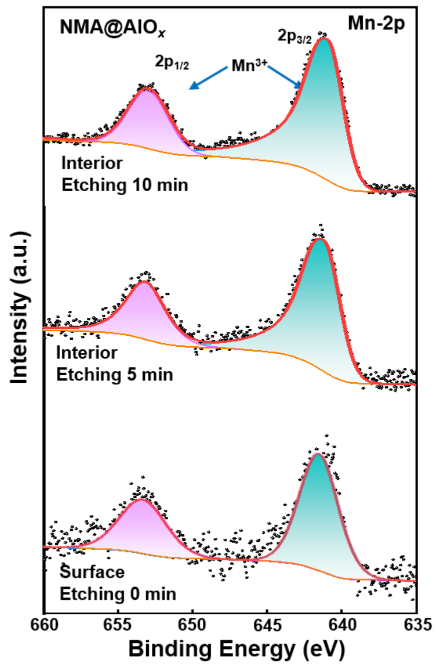

Figure S4. XPS spectra of Mn-2p peaks of NMA@ AlO_x with different etching time.

Pristine, etching 5 min and etching 10 min (from down to top).

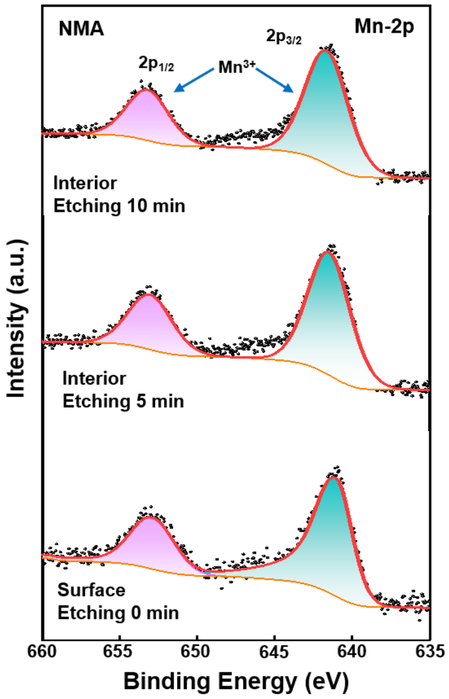

Figure S5. XPS spectra of Mn-2p peaks of NMA with different etching time. Pristine, etching 5 min and etching 10 min (from down to top).

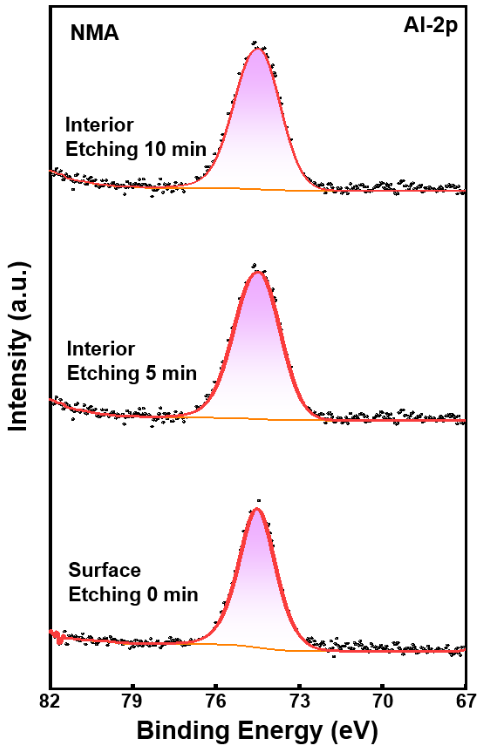

Figure S6. XPS spectra of Al-2p peaks of NMA with different etching time. Pristine, etching 5 min and etching 10 min (from down to top).

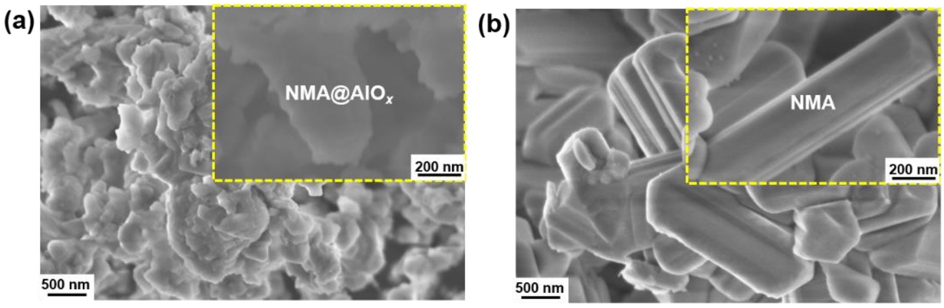

Figure S7. SEM images of NMA@AlO$_x$ (a) and NMA (b).

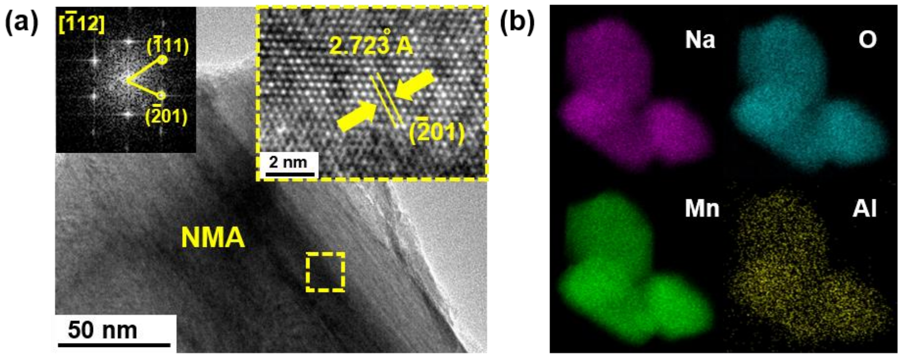

Figure S8. HRTEM image (insert, FFT image and corresponding Bragg spots) (a) and TEM-EDS mappings (b) images of NMA.

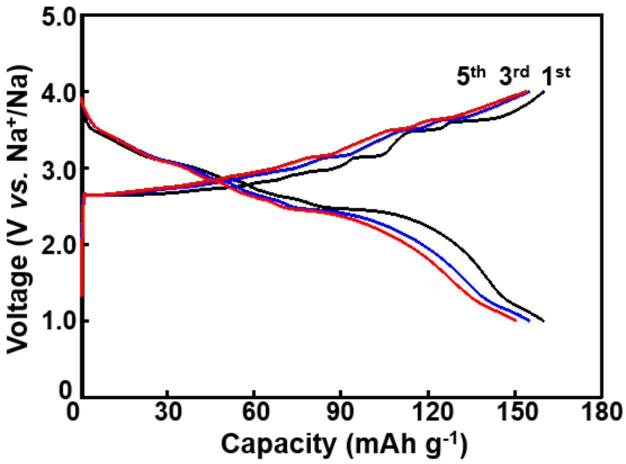

Figure S9. Charge-discharge curves of NMA at 20 mA g^{-1}.

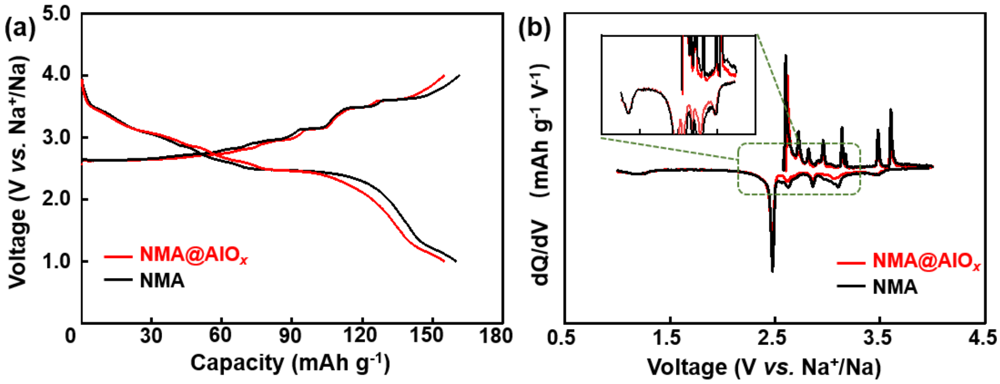

Figure S10. First Charge-discharge curves of NMA@AlO_x and NMA at 20 mA g^{-1} (a) and dQ/dV versus voltage of NMA@AlO_x and NMA cathodes at 20 mA g^{-1} (inset, partial enlarge curves) (b).

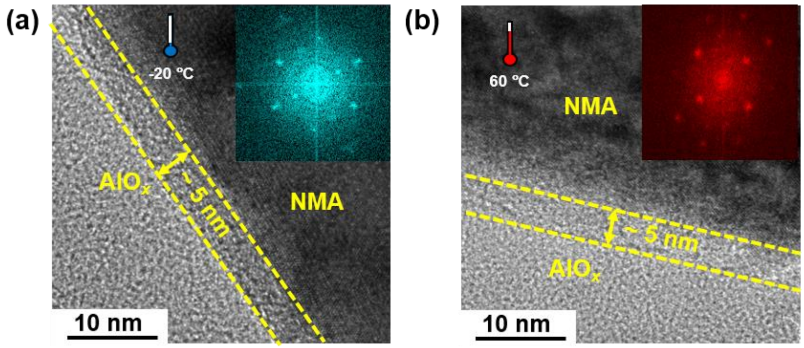

Figure S11. TEM images of NMA@AlO_x after cycled at -20 °C (a) and 60°C (b) (insert, SAED patterns).

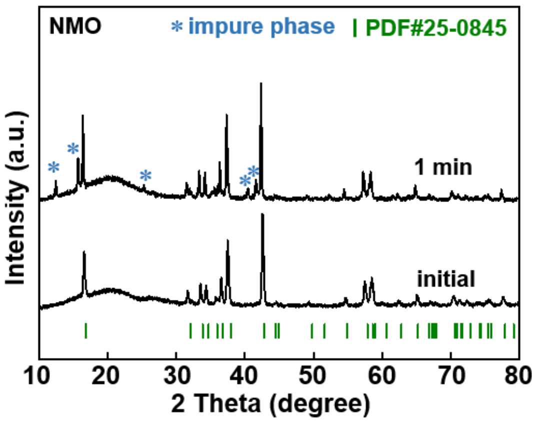

Figure S12. XRD patterns of initial NMO and NMO exposed at air for 1 min.

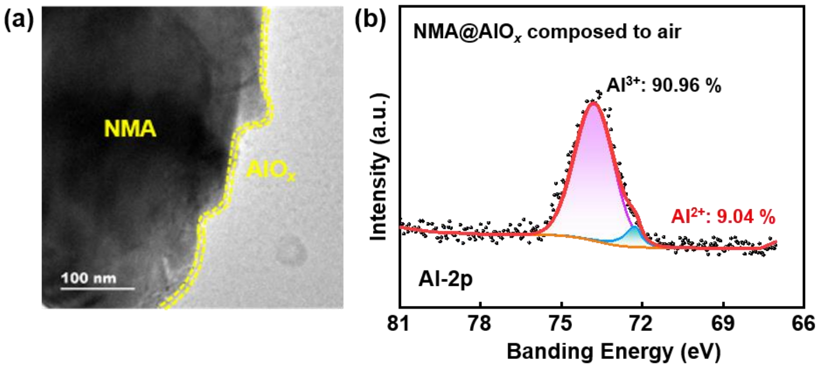

Figure S13. TEM image (a) and XPS spectrum of the exposed NMA@AlO_x sample.

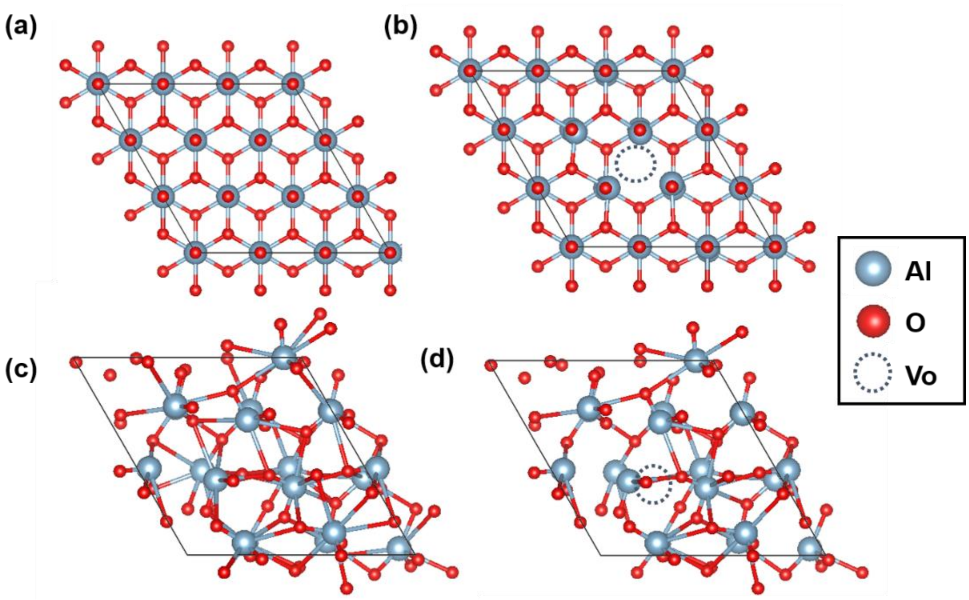

Figure S14. Modeling crystal structure diagram of crystalline Al_2O_3 (c-Al_2O_3) (a), crystalline $AlO_{1.45}$ (c-$AlO_{1.45}$) (b), amorphous Al_2O_3 (a-Al_2O_3) (c)and amorphous $AlO_{1.45}$ (a-$AlO_{1.45}$) (d).

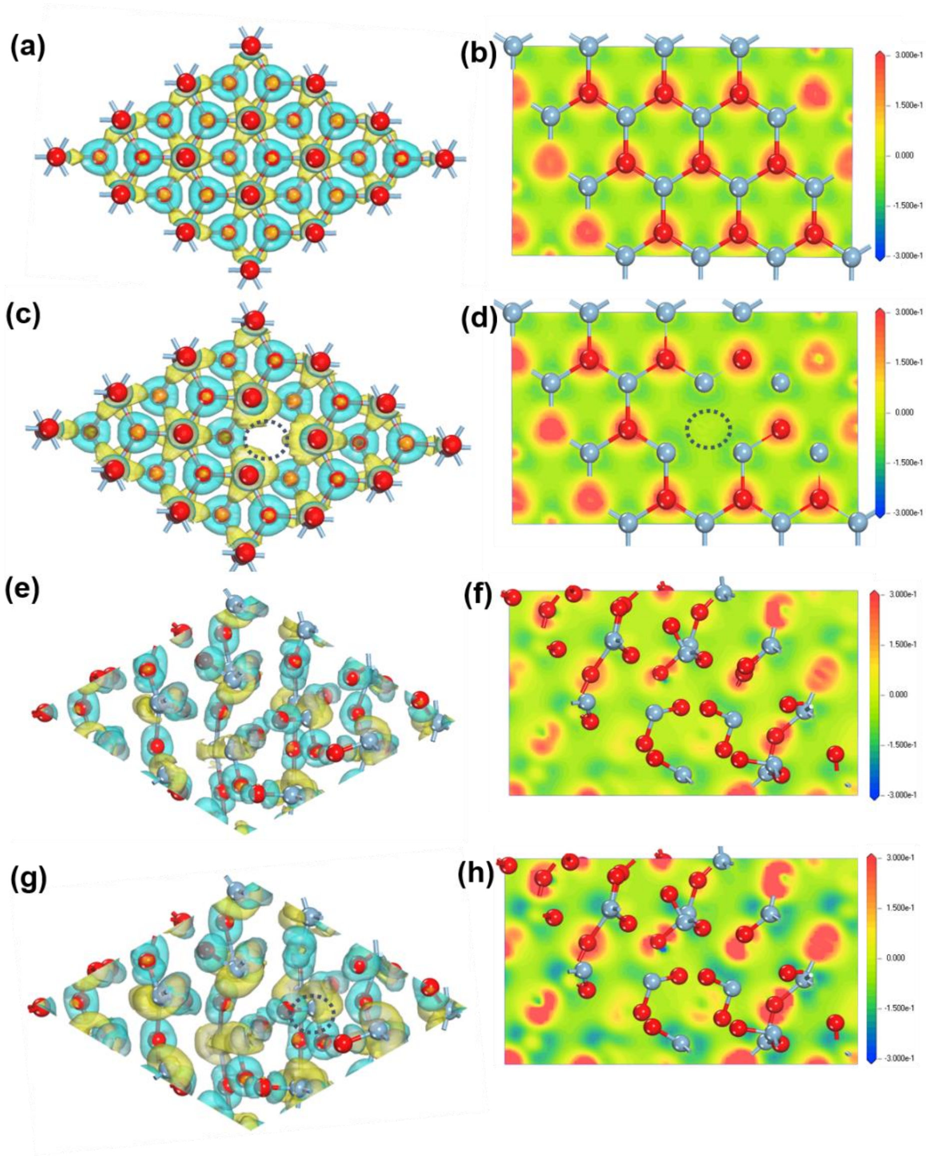

Figure S15. Charge density distribution images of crystalline Al_2O_3 (a, b), crystalline $AlO_{1.45}$ (c, d), amorphous Al_2O_3 (e, f) and amorphous $AlO_{1.45}$ (g, h).

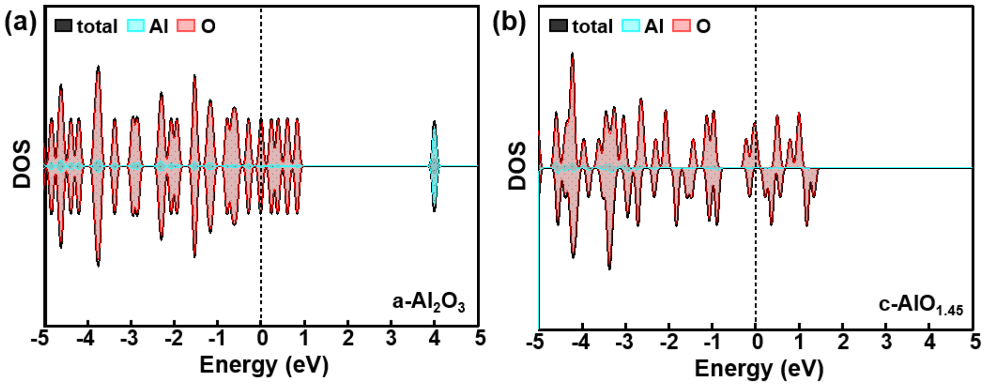

Figure S16. DOS curves of amorphous Al_2O_3 (a) and crystalline $AlO_{1.45}$.

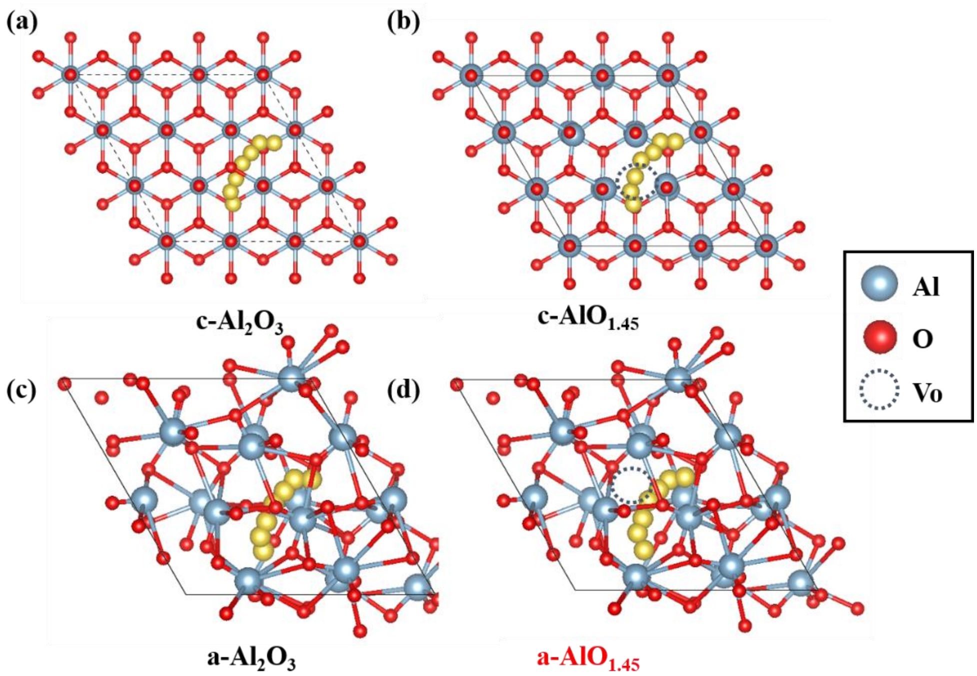

Figure S17. Modeling diagram of Na^+ diffusion. crystalline Al_2O_3 (c-Al_2O_3) (a), crystalline $AlO_{1.45}$ (c-$AlO_{1.45}$) (b), amorphous Al_2O_3 (a-Al_2O_3) (c)and amorphous $AlO_{1.45}$ (a-$AlO_{1.45}$) (d).

Table S1. EIS Fitting results of NMA and NMA@AlO_x at different temperatures

T (°C)	NMA			NMA@AlO_x		
	R_s (Ω)	R_{ct} (Ω)	D_{Na+} (cm^2 s^{-1})	R_s (Ω)	R_{ct} (Ω)	D_{Na+} (cm^2 s^{-1})
-20	3.575	2148	1.521×10^{-15}	2.557	324.6	1.954×10^{-14}
25	2.379	685.5	2.031×10^{-13}	2.258	272	2.207×10^{-13}
60	1.822	279.3	1.386×10^{-13}	1.441	141.3	1.271×10^{-12}

Table S2. Tap-Density data of NMA and NMA@AlO_x

Item	NMA	NMA@AlO_x
RPM	250 rpm	250 rpm
Tap-Density (g cm^{-3})	1.16	1.22
Hausner Ratio	1.11	1.40
Compression index	10.00 %	28.57 %

Table S3. ICP results of Mn element on Na anode surface of different cells

cells	Mn contents (ppm)
Na/NMA half cell	0.00
250 th cycled Na/NMA half cell	~0.75
Na/NMA@AlO$_x$ half cell	0.00
250 th cycled Na/NMA@AlO$_x$ half cell	0.00

Table S4 Comparison of this work and other related work in literatures

Chemical formula	Coating layer	Specific capacity	Practical/ Theoretical	Rate	Cycle	T (°C)	Literature
P2-$Na_{2/3}[Ni_{1/3}Mn_{2/3}]O_2$	Al_2O_3 12 nm	164 mAh g^{-1}	86.3	160 mAh g^{-1}~60 mAh g^{-1} (C/20~10 C)	200 cycles, 79.2 % （10 C）	25	*[1]*
P2-$Na_{0.5}Mn_{0.5}Co_{0.5}O_2$	Al_2O_3 3 nm	154 mAh g^{-1}	67.7%	174 mAh g^{-1}~45 mAh g^{-1} (1/30 C~1/10 C)	100 cycles, 80 % （10/C）	25	*[2]*
P2–$Na_{0.67}MnO_2$	Al_2O_3 3 nm	134 mAh g^{-1}	78.3 %	156 mAh g^{-1}~103 mAh g^{-1} (1/30 C~1/10 C)	200 cycles, 74.1 % （0.1 C）	25	*[3]*
P2$Na_{2/3}[Ni_{1/3}Mn_{2/3}]O_2$	CuO 5 nm	107 mAh g^{-1}	56.3 %	107 mAh g^{-1}~70 mAh g^{-1} (1/30 C~1/10 C)	20 cycles, 48.6% （0.1 C）	25	*[4]*
P2-$Na_{0.5}Ni_{0.33}Mn_{0.67}O_2$	MgO 1.3 nm	131 mAh g^{-1}	68.9%	131 mAh g^{-1}~51 mAh g^{-1} (1/30 C~1/10 C)	100 cycles, 83 %	25	*[5]*
$Na[Ni_{0.5}Mn_{0.5}]O_2$	MgO 100 nm	167 mAh g^{-1}	87.9%	167 mAh g^{-1}~100 mAh g^{-1} (1/30 C~1/10 C)	200 cycles, 70 % （0.1 C）	25	*[6]*
$Na_{0.67}[Ni_{0.5}Fe_{0.5}]O_2$	MgO 10 nm	187 mAh g^{-1}	72.8%	187 mAh g^{-1}~87 mAh g^{-1} (12 mA g^{-1}~480 mA g^{-1})	100cycles，72 % （0.05 C）	25	*[7]*
$NaMn_{0.6}Al_{0.4}O_2$	AlO_x 5nm	155 mAh g^{-1}	98.1%	155 mAh g^{-1}~104 mAh g^{-1} (20 mA g^{-1}~1000 mA g^{-1})	250 cycles, 81 %	-20~60	*This work*

References

[1] Y. Liu, X. Fang, A. Zhang, C. Shen, Q. Liu, H. A. Enaya, C. Zhou, Layered P2-$Na_{2/3}[Ni_{1/3}Mn_{2/3}]O_2$ as high-voltage cathode for sodium-ion batteries: The capacity decay mechanism and Al_2O_3 surface modification, Nano Energy 27 (2016) 27-34.

[2] H. V. Ramasamy, P. N. Didwal, S. Sinha, V. Aravindan, J. Heo, C.-J. Park, Y.-S. Lee, Atomic layer deposition of Al_2O_3 on P2-$Na_{0.5}Mn_{0.5}Co_{0.5}O_2$ as interfacial layer for high power sodium-ion batteries, J. Colloid Interface Sci. 564 (2020) 467-477.

[3] W. Zuo, J. Qiu, X. Liu, B. Zheng, Y. Zhao, J. Li, H. He, K. Zhou, Z. Xiao, Q. Li, G. F. Ortiz, Y. Yang, Highly-stable P2-$Na_{0.67}MnO_2$ electrode enabled by lattice tailoring and surface engineering, Energy Stor. Mater. 26 (2020) 503-512.

[4] R. Dang, Q. Li, M. Chen, Z. Hu, X. Xiao, CuO-coated and Cu^{2+}-doped Co-modified P2-type $Na_{2/3}[Ni_{1/3}Mn_{2/3}]O_2$ for sodium-ion batteries, Phys. Chem. Chem. Phys. 21 (2019) 314-321.

[5] H. V. Ramasamy, K. Kaliyappan, R. Thangavel, V. Aravindan, K. Kang, D. U. Kim, Y. Park, X. Sun, Y.-S. Lee, Cu-doped P2-$Na_{0.5}Ni_{0.33}Mn_{0.67}O_2$ encapsulated with MgO as a novel high voltage cathode with enhanced Na-storage properties, J. Mater. Chem. A 5 (2017) 8408-8415.

[6] J.-Y. Hwang, T.-Y. Yu, Y.-K. Sun, Simultaneous MgO coating and Mg doping of $Na[Ni_{0.5}Mn_{0.5}]O_2$ cathode: facile and customizable approach to high-voltage sodium-ion batteries, J. Mater. Chem. A 6 (2018) 16854-16862.

[7] W. Kong, H. Wang, L. Sun, C. Su, X. Liu, Understanding the synergic roles of MgO coating on the cycling and rate performance of $Na_{0.67}Mn_{0.5}Fe_{0.5}O_2$ cathode, Appl. Surf. Sci. 497 (2019) 143841.